

Effect of magnetic field on jet transport coefficient \hat{q}

Debjani Banerjee¹, Souvik Paul², Prottoy Das¹, Abhi Modak¹, Ankita Budhraja³,
Sabyasachi Ghosh⁴, and Sidharth K. Prasad¹

¹Department of Physics, Bose Institute, EN 80, Sector-V, Salt Lake, Kolkata - 700091, WB, India

²Department of Physical Sciences, Indian Institute of Science Education and Research, Kolkata, Mohanpur, West Bengal 741246, India

³Tata Institute of Fundamental Research, Homi Bhabha Road, Colaba, Mumbai 400005, Maharashtra, India

⁴Indian Institute of Technology Bhilai, GEC Campus, Sejbahar, Raipur 492015, Chhattisgarh, India

Abstract

We report the effect of magnetic field on estimation of jet transport coefficient, \hat{q} using a simplified quasi-particle model. Our adopted quasi-particle model introduces temperature and magnetic field dependent degeneracy factors of partons, which are tuned by fitting the magnetothermodynamical data of lattice quantum chromodynamics. In absence of magnetic field, \hat{q} is estimated by using the temperature dependent degeneracy factor. At finite magnetic field, \hat{q} splits into parallel and perpendicular components, whose magnetic field dependent part has two sources. One is field dependent degeneracy factor and another is phase space part, guided from shear viscosity to entropy density ratio. Their collective role provides an enhanced jet transport coefficients, which should be considered in detailed jet quenching phenomenology in presence of magnetic field.

1 Introduction

In high energy hadron-hadron, hadron-nucleus and nucleus-nucleus collisions, partons produced in large-momentum transfer (large Q^2) processes, undergo multiple fragmentations (forming shower of partons) and form a collimated spray of energetic colorless hadrons (due to color charge confinement property of quantum chromodynamics (QCD)) known as jets [1]. The production and properties of jets in vacuum (e.g. in proton-proton (pp) and in proton-nucleus (pA)) can be very well understood within the theoretical framework of perturbative quantum chromodynamics (pQCD) [2–7]. Jets are produced very early in the collision due to their small formation time [8, 9]. In nucleus-nucleus (AA) collisions, where a thermalized (expanding) medium - quark gluon plasma (QGP) is produced, these jets lose their energy via elastic and inelastic interactions with the medium partons while passing through it resulting in the suppression of high energy jets in AA collisions relative to that in pp and pA collisions. The phenomenon is known as jet quenching [10–13] and can be quantified experimentally by a well known observable, nuclear modification factor R_{AA} , defined as the ratio of high momentum inclusive hadron or jet yields in AA collisions to that in N_{coll} (number of binary collisions) scaled pp collisions. The suppression of high momentum hadrons and jets are experimentally measured previously by experiments at SPS, RHIC and recently by experiments at LHC [14–18]. Within the framework of theoretical models, jet quenching can be studied to extract

and put constrain on the jet transport coefficient \hat{q} of the QGP which is defined as the mean square of the momentum transfer between the propagating hard jet and the soft medium per unit length.

There are different theoretical models [13], popularly known as GLV-CUJET [19–21], MARTINI [22], MCGILL-AMY [23], HT-M [12, 24], HT-BW [25–27], which have well explored this jet quenching phenomena by calculating the theoretical quantity \hat{q} and then proceed for experimental quantity R_{AA} . In evolution of bulk medium, different models follow different strategy but for jet-medium interaction, they have considered pQCD calculations. In GLV-CUJET model [19–21], an effective quark-gluon cross section in terms of strong coupling constant, electric and magnetic screening mass is used. MARTINI [22] and MCGILL-AMY [23] models have considered hard thermal loop (HTL) based resummed elastic collision rate. HT-M [12, 24], HT-BW [25–27] models grossly assume \hat{q} as proportional to (local) entropy or number density by normalizing with its cold nuclear matter value $\hat{q}_N \approx 0.02 \text{ GeV}^2/\text{fm}$ [28, 29] and its initial values \hat{q}_0 . To explain PHENIX data [30], Ref. [27] has found $\hat{q}_0 \approx 0.9 \text{ GeV}^2/\text{fm}$. Others possible values [13] are found as $\hat{q}_0 \approx 1.2 \text{ GeV}^2/\text{fm}$ to explain PHENIX data [30, 31][77,78] and $\hat{q}_0 \approx 2.2 \text{ GeV}^2/\text{fm}$ to explain combined ALICE [32] and CMS [33]. Collecting those different possible values of \hat{q} , we will get a numerical range [13], which may be well accepted.

Present article is intended to explore the role of magnetic field on this jet quenching parameter as as RHIC or LHC matter may face $eB = 1 - 10 m_\pi^2$ magnetic field in non-central collisions [34]. Hence, without going to microscopic calculation of \hat{q} in absence of magnetic field, here we have calibrated it with existing known values and then extended it for finite magnetic field picture. Following Ref. [27], firstly we have attempted to map the transition from \hat{q}_0 to \hat{q}_N through a quasi-particle type description [35], based on lattice QCD (LQCD) thermodynamics [36, 37]. Latter it is extended for finite magnetic field picture based on the LQCD magneto-thermodynamics [38, 39]. Similar kind of magnetic field extension of quasi-particle models are addressed by Refs. [40–43], based on effective QCD models. In that context, our approach is not at all so rich to deal with effective dynamics but an easy-dealing parametric based model to map LQCD magneto-thermodynamics, which has revealed inverse magnetic catalysis (IMC) property of quark-hadron phase transition in presence of magnetic field. To add anisotropic phase-space part at finite temperature T and magnetic field B into the \hat{q} , we take the help of shear viscosity η expression in presence of magnetic field since \hat{q} and η can be connected [44–49]. Our investigation focuses mainly on observing the changes in the value of jet quenching parameter due to magnetic field, which is found to be quite noticeable.

The present article is organized as follows. Sec. 2 describes the mapping of LQCD thermodynamic quantities in presence of magnetic field by introducing temperature and magnetic field dependent degeneracy factor. The formalism to estimate jet quenching parameter using quasi-particle description is discussed in Sec. 3. In Sec. 4, we have attempted to calculate magnetic field dependent jet quenching parameter using the knowledge of temperature and magnetic field dependent phase space part of shear viscosity. The obtained results in this work are discussed in Sec. 5 and the comparison with non-perturbative toolbox of AdS/CFT results is outlined in Sec. 6. Finally, we conclude with a summary in Sec. 7.

2 Mapping LQCD magneto-thermodynamics

This section is aimed to map LQCD thermodynamics, which will be used to calculate \hat{q} in Sec.(3). For mapping LQCD thermodynamics, we will follow the steps of Ref. [35], which is basically attempted to map LQCD thermodynamics of Refs. [36, 37]. Here, we will attempt to map LQCD thermodynamics in presence of magnetic field, given by Ref. [39], but following the same steps, adopted in Ref. [35].

In terms of Fermi-Dirac (FD) distribution function of quarks and Bose-Einstein (BE) distribution function of gluons, the energy density and pressure of QGP system can be expressed as

$$\epsilon_{QGP} = g_g \int_0^\infty \frac{d^3\vec{k}}{(2\pi)^3} \frac{\omega_g}{e^{\beta\omega_g} - 1} + g_Q \int_0^\infty \frac{d^3\vec{k}}{(2\pi)^3} \frac{\omega_Q}{e^{\beta\omega_Q} + 1} \quad (1)$$

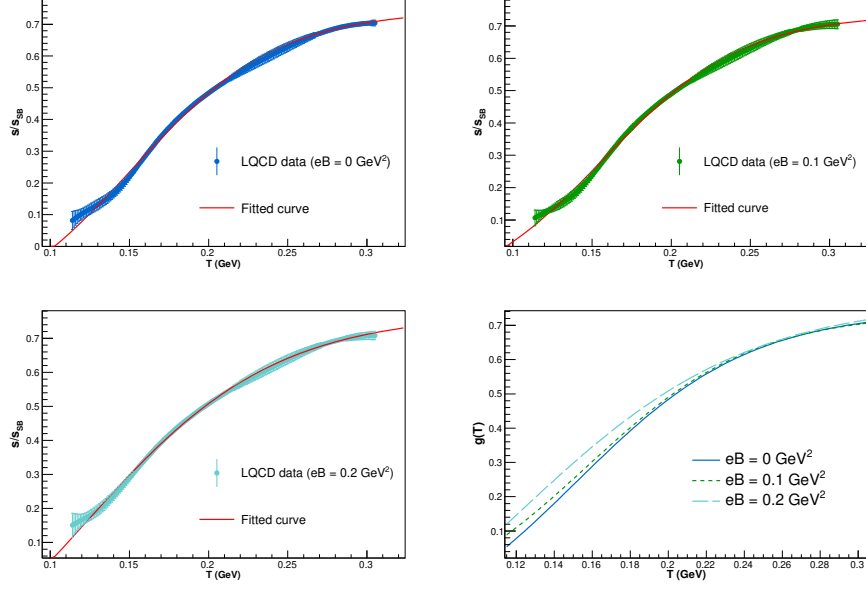


Figure 1: LQCD data points (points with error bars) [39] and fitted curves (solid line) of normalized entropy density, normalized by its SB limit (s/s_{SB}) vs T at $eB = 0$ (left-upper panel), $eB = 0.1 \text{ GeV}^2$ (right-upper panel) and $eB = 0.2 \text{ GeV}^2$ (left-lower panel). Right-lower panel : Corresponding T dependent fraction $g(T)$, multiplied with total degeneracy factor at different eB .

and

$$P_{QGP} = g_g \int_0^\infty \frac{d^3\vec{k}}{(2\pi)^3} \left(\frac{\vec{k}^2}{3\omega_g} \right) \frac{1}{e^{\beta\omega_g} - 1} + g_Q \int_0^\infty \frac{d^3\vec{k}}{(2\pi)^3} \left(\frac{\vec{k}^2}{3\omega_Q} \right) \frac{1}{e^{\beta\omega_Q} + 1} , \quad (2)$$

where ω_Q, ω_g are energies and

$$\begin{aligned} g_Q &= (\text{spin}) \times (\text{particle/anti particle}) \times (\text{color}) \times (\text{flavor}) = 2 \times 2 \times 3 \times 3 = 36 , \\ g_g &= (\text{spin}) \times (\text{flavor}) = 2 \times 8 = 16 , \end{aligned} \quad (3)$$

are degeneracy factors of quarks and gluons respectively. At zero net quark density or quark chemical potential, entropy density can be expressed in terms of P and ϵ as

$$s_{QGP} = \frac{P_{QGP} + \epsilon_{QGP}}{T} . \quad (4)$$

For massless QGP system,

$$\begin{aligned} P_{QGP} &= \left[g_g + g_Q \left(\frac{7}{8} \right) \right] \frac{\pi^2}{90} T^4 \approx 5.2 T^4 , \\ \epsilon_{QGP} &= \left[g_g + g_Q \left(\frac{7}{8} \right) \right] \frac{3\pi^2}{90} T^4 \approx 15.6 T^4 , \\ s_{QGP} &= \left[g_g + g_Q \left(\frac{7}{8} \right) \right] \frac{4\pi^2}{90} T^3 \approx 20.8 T^3 . \end{aligned} \quad (5)$$

Now, if we see the LQCD data of $P(T)$, $\epsilon(T)$, $s(T)$ at $eB = 0$ from Ref. [39], then one can notice that the data points always remain lower than their massless limits i.e. $\frac{P}{T^4} < 5.2$, $\frac{\epsilon}{T^4} < 15.6$, $\frac{s}{T^3} < 20.8$.

Table 1: Different values of $a_{0,1,2,3}$ given in Eq. (7) for different magnetic field strengths

$eB(\text{GeV}^2)$	a_0	a_1	a_2	a_3
0.0	-0.26	-1.49	-21.58	1.49
0.1	-0.16	-1.20	-22.61	1.33
0.2	-0.47	-2.82	-16.51	2.26

A rich QCD interaction in non-perturbative domain is responsible for this suppression and it is LQCD calculation which provides useful insights in this domain, where pQCD does not work well. One can map these temperature (T) dependent suppression of $P(T)$, $\epsilon(T)$, $s(T)$ [35] by imposing a temperature dependent fraction $g(T)$, multiplied with the total degeneracy factor of QGP. So, this picture assumes that as we go from high temperature to low temperature, the degeneracy factor of massless QGP system is gradually reduced.

Now, let us proceed with a finite magnetic field picture. In presence of magnetic field along z-axis, we can get an anisotropy in pressure but if we consider the pressure along z-direction (P_z), then the thermodynamic relation

$$s = \frac{\epsilon + P_z}{T} \quad (6)$$

remains same [38]. So, the earlier expressions can still be used for finite B picture by introducing a T , B dependent parameter $g(T, B)$. By matching LQCD data of Bali et. al. [38, 39], who have provided $P(T, B)$, $\epsilon(T, B)$, $s(T, B)$ one can get the parametric form of $g(T, B)$ as

$$g(T, B) = a_0 - \frac{a_1}{e^{a_2(T-0.17)} + a_3} , \quad (7)$$

where values of $a_{0,1,2,3}$ for different eB 's are given in Tab.1.

Now, an exact (quantitative) matching of all the LQCD thermodynamical quantities through a single parameter tuning is probably an impossible task. In this context, our mapping might not be considered as so robust but can surely be considered as a simplified and easy-dealing tool. Since it is difficult for exact fitting of P , ϵ and s simultaneously via a single set of $g(T, B)$, therefore, we have to focus on any one of them for exact fitting, doing which a little bad fitting of the remaining thermodynamical quantities can be expected. Among all the thermodynamical quantities, we have chosen entropy density as our one of the aim is to estimate η/s later.

3 Jet quenching parameter

Following Ref. [27], the jet quenching parameter of hadronic matter can be proportionally related to its density as:

$$\hat{q}(T) = \frac{\hat{q}_N}{\rho_N} \rho_h(T) , \quad (8)$$

where $\hat{q}_N \approx 0.02 \text{ GeV}^2/\text{fm}$ [28, 29] is the jet transport parameter at the center of the cold nuclear matter in a large nucleus, $\rho_N = 0.17 \text{ fm}^{-3}$ is nuclear saturation density and ρ_h is hadronic matter density. In Ref. [27], $\rho_h(T)$ is obtained from hadron resonance gas (HRG) model within the hadronic temperature range. As an alternative way, here we have replaced $\rho_h(T)$ by $\rho_G(T)$, which is density of gluon and it can be extended beyond (quark-hadron) transition temperature. The $\rho_G(T)$ can be calculated by using $g(T)$, as we did for other thermodynamical quantities for QGP. Similar to Eqs (1), (2) etc., the gluon number density ρ_G can be expressed as

$$\rho_G = g_g \int_0^\infty \frac{d^3\vec{k}}{(2\pi)^3} \frac{1}{e^{\beta\omega_g} - 1} , \quad (9)$$

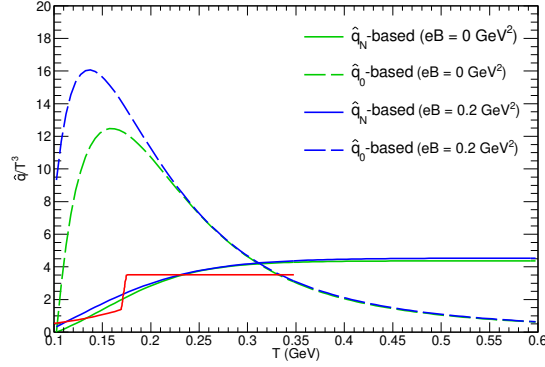


Figure 2: \hat{q}/T^3 by using Eq. (11) (green solid line) and Eq. (13) (green dash line) for $eB = 0$. \hat{q}/T^3 by using $g(T, eB = 0.2 \text{ GeV}^2)$ in Eq. (11) (blue solid line) and Eq. (13) (blue dash line) for $eB = 0.2 \text{ GeV}^2$.

whose massless limit will be

$$\begin{aligned} \rho_G &= \left[g_g \frac{\zeta(3)}{\pi^2} \right] T^3 \\ &= 1.94 T^3. \end{aligned} \quad (10)$$

When this massless gluon density will be multiplied with $g(T)$, then one may get a rough estimation of gluon density in non-pQCD domain. So, Eq. (8) can be converted as

$$\begin{aligned} \hat{q}(T) &= \frac{\hat{q}_N}{\rho_N} \times g(T) \times g_g \frac{\zeta(3)}{\pi^2} T^3 \\ &= 3.03 \times \left[a_0 - \frac{a_1}{e^{a_2(T-0.17)} + a_3} \right] \times 1.94 T^3 \end{aligned} \quad (11)$$

The above equation is calibrated by cold nuclear matter data and journey is from hadronic (low) to QGP (high) temperature domain. The information of LQCD thermodynamics carried via $g(T)$ may result in a cross-over type transition in $\hat{q}(T)$. The green solid line of Fig. (2) exposes it when we compare to first order phase transition type or discrete type curve taken from Ref. [27]. Since Ref. [27] has considered \hat{q} in hadronic temperature range with density from hadron resonance gas (HRG) model and $\hat{q}_0 \approx 0.9 \text{ GeV}^2/\text{fm}$ (jet transport parameter at initial time of QGP) in quark temperature range, therefore, a discrete pattern in \hat{q}/T^3 is seen. One can find that HRG estimation of Ref. [27] and our estimation in hadronic temperature range are quite comparable. However, our extended estimation in quark temperature range saturates around 4.5 ($\sim T = 0.370 \text{ GeV}$), which is close to the corresponding initial value – $\hat{q}_0/T^3 = 0.9 \times 0.197/(0.370^3) \approx 3.46$ [27].

Next, a reverse journey from high to low temperature domain is also possible, where $\hat{q}_0 \approx 0.9 \text{ GeV}^2/\text{fm}$ at initial time will be our reference point. Assuming an equivalence between \hat{q}_0 and massless limit of \hat{q} :

$$\begin{aligned} \hat{q}_{m=0} &= \lim_{m \rightarrow 0} \hat{q}(T) = \frac{\hat{q}_N}{\rho_N} 16 \frac{\zeta(3)}{\pi^2} T^3 \\ &\approx 5.87 \times T^3, \end{aligned} \quad (12)$$

we can redefine Eq. (8) as

$$\begin{aligned}
\hat{q}(T) &= \frac{\hat{q}_N}{\rho_N} \rho_h(T) \left(\frac{\hat{q}_0}{\hat{q}_{m=0}} \right) \\
&= g(T) \times \hat{q}_0 \\
&= \left[a_0 - \frac{a_1}{e^{a_2(T-0.17)} + a_3} \right] \times 0.9 \text{ GeV}^2/\text{fm} .
\end{aligned} \tag{13}$$

The green dash line curve in Fig. (2), based on Eq. (13), is never crossing the estimation corresponding to initial value $\hat{q}_0 \approx 0.9 \text{ GeV}^2/\text{fm}$. One should notice that it saturates below the pQCD-based value $\hat{q}_0 \approx 0.9 \text{ GeV}^2/\text{fm}$. One can find a similar kind of picture where LQCD values of different thermodynamical quantities always saturate around a smaller values of their corresponding SB limits or leading order pQCD values. This equivalence between LQCD thermodynamics and jet quenching parameter is coming through the concept of temperature dependent degeneracy factor [35].

So, either by using Eq. (11) or Eq. (13), one can go for a rough estimation of $\hat{q}(T)$. Interestingly, \hat{q}/T^3 from Eq. (13) show a mild peak structure near transition temperature, as shown by green dash line in Fig. (2). Analyzing T dependency of Eq. (11) and Eq. (13), one can recognize $\hat{q} \propto g(T) \times T^3$ and $\hat{q} \propto g(T)$ respectively, so their normalizing function will be $\frac{\hat{q}}{T^3} \propto g(T)$ and $\frac{\hat{q}}{T^3} \propto \frac{g(T)}{T^3}$ respectively. It is due to the collective roles of increasing $g(T)$ and decreasing $\frac{1}{T^3}$, the peak structure is forming.

One can also be able to estimate $\hat{q}(T, B)$ by using finite B extension of our quasi-particle model, which has fitted LQCD IMC data via simple parametric form of T and B dependent degeneracy factor $g(T, B)$. Replacing $g(T)$ by $g(T, B)$ in Eq. (11) and Eq. (13) for $eB = 0.2 \text{ GeV}^2$, we have obtained black dotted and pink dash-dotted curves respectively. However, this straight forward extension in finite B case might not be a complete picture. Similar to other transport coefficients, jet transport parameter can have a T, B dependent phase space part, which is not yet considered. In the next section, we have attempted to include this structure.

4 Phase space component

According to Refs. [44–48], jet quenching parameter is connected with the shear viscosity coefficient. Here, we make an attempt to calculate $\hat{q}(T, B)$ from the knowledge of $\eta(T, B)$ profile. The advantage of this approach lies in the fact that the T, B dependent phase space part of $\eta(T, B)$ are well studied in recent Refs. [50–63]. So based on that knowledge, we have invoked the T, B dependent phase space part into $\hat{q}(T, B)$.

Let us take a quick revisit of shear viscosity expressions at finite temperature and magnetic field. We first consider the case of zero magnetic field, then we move to the non-zero magnetic field picture. According to the macroscopic fluid definition, shear viscosity η is the proportionality constant between viscous stress tensor π_{ij} and velocity gradient tensor C_{ij} [63], i.e.

$$\pi^{ij} = \eta C_{ij} , \tag{14}$$

which is relativistic and tensor form of the so-called Newton's law of viscosity. In microscopic kinetic theory approach, the viscous stress tensor can be connected with the deviation (from equilibrium distribution function f_0) $\delta f = C k^k k^l C_{kl} \beta f_0 (1 \mp f_0)$ as

$$\begin{aligned}
\pi^{ij} &= g \int \frac{d^3 \vec{k}}{(2\pi)^3} \frac{k^i k^j}{\omega} \delta f \\
&= g \int \frac{d^3 \vec{k}}{(2\pi)^3} \frac{k^i k^j}{\omega} C k^k k^l C_{kl} \beta f_0 (1 - a f_0) ,
\end{aligned} \tag{15}$$

where $f_0 = 1/[e^{\beta\omega} + a]$ denotes the Fermi-Dirac (FD) and Bose-Einstein (BE) distribution functions for $a = \pm 1$ respectively and $\omega = \sqrt{\vec{k}^2 + m^2}$ is the energy of medium constituent with mass m and degeneracy factor g .

Connecting the macroscopic Eq. (14) and microscopic Eq. (15), we can get the shear viscosity tensor:

$$\eta^{ijkl} = g \int \frac{d^3\vec{k}}{(2\pi)^3} \frac{k^i k^j k^k k^l}{\omega^2} \tau_c \beta f_0 (1 - a f_0) , \quad (16)$$

whose isotropic expression will be

$$\eta = \frac{g}{15} \int \frac{d^3\vec{k}}{(2\pi)^3} \frac{\vec{k}^4}{\omega^2} \tau_c \beta f_0 (1 - a f_0) , \quad (17)$$

The unknown constant C in Eq. (15) has been obtained in terms of relaxation time τ_c with the help of relaxation time approximation (RTA) based relativistic Boltzmann equation (RBE) [63].

Now, in presence of magnetic field, instead of a single traceless velocity gradient tensor C_{ij} , we will get 5 independent traceless tensors - one set is proposed in Ref. [50] and another set is proposed by Refs. [51, 52]. Therefore, we will get two sets of 5 shear viscosity components $\tilde{\eta}_{0,1,2,3,4}$ [55, 59, 63] and $\eta_{0,1,2,3,4}$ [61, 63]. They are interconnected and the two main components with respect to the direction of applied magnetic field are as follows:

$$\begin{aligned} \frac{\eta_{\parallel}}{\eta} &= \frac{\tilde{\eta}_2}{\eta} = \frac{(\eta_0 + \eta_2)}{\eta} = \frac{1}{1 + (\tau_c/\tau_B)^2} \\ \frac{\eta_{\perp}}{\eta} &= \frac{\tilde{\eta}_1}{\eta} = \frac{\eta_0}{\eta} = \frac{1}{1 + 4(\tau_c/\tau_B)^2} , \end{aligned} \quad (18)$$

where another time scale $\tau_B = \frac{\omega_{av}}{qB}$ (ω_{av} is the average energy) will come into the picture along with relaxation time τ_c . In massless limit,

$$\begin{aligned} \omega_{av} &= \left\{ \frac{\zeta(4)}{\zeta(3)} \right\} 3T \text{ for BE} \\ &= \left\{ \frac{7\zeta(4)}{2\zeta(3)} \right\} 3T \text{ for FD} , \end{aligned} \quad (19)$$

and

$$\begin{aligned} \eta &= \frac{4g}{5\pi^2} \zeta(4) T^4 \text{ for BE} \\ &= \left(\frac{7}{8} \right) \frac{4g}{5\pi^2} \zeta(4) T^4 \text{ for FD} . \end{aligned} \quad (20)$$

Now, for massless 3 flavor QGP at $B = 0$, we can get

$$\begin{aligned} \eta &= \left[16 + \frac{7}{8} 36 \right] \frac{4}{5\pi^2} \zeta(4) T^4 , \\ s &= \left[16 + \frac{7}{8} 36 \right] \frac{4}{\pi^2} \zeta(4) T^3 , \\ \Rightarrow \frac{\eta}{s} &= \frac{\tau_c T}{5} . \end{aligned} \quad (21)$$

For $B \neq 0$, we get

$$\begin{aligned} \frac{\eta_{\parallel}}{s} &= \frac{1}{\left[16 + \frac{7}{8} 36 \right]} \left[16 + \frac{7}{8} 12 \sum_{u,d,s} \frac{1}{1 + (\tau_c/\tau_B)^2} \right] \frac{\tau_c T}{5} \\ \frac{\eta_{\perp}}{s} &= \frac{1}{\left[16 + \frac{7}{8} 36 \right]} \left[16 + \frac{7}{8} 12 \sum_{u,d,s} \frac{1}{1 + 4(\tau_c/\tau_B)^2} \right] \frac{\tau_c T}{5} . \end{aligned} \quad (22)$$

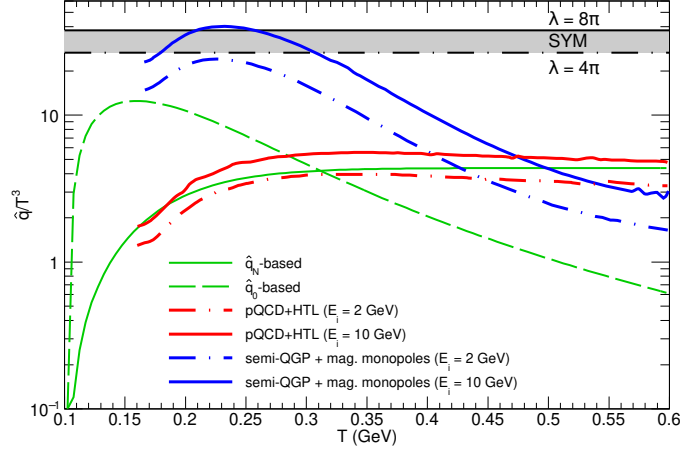


Figure 3: Dependence of \hat{q}/T^3 on temperature (T in GeV) in absence of magnetic field — estimations based on \hat{q}_N (green solid line) and \hat{q}_0 (green dashed line), pQCD + HTL approach for quark jet of initial energy $E_i = 2$ GeV (red dash-dotted line) and $E_i = 10$ GeV (red solid line) and semi-QGP + magnetic monopoles approach for $E_i = 2$ GeV (blue dash-dotted line) and $E_i = 10$ GeV (blue solid line). Black dash-dotted and solid lines represent \hat{q} of an isotropic $\mathcal{N} = 4$ SYM plasma at zero magnetic field for $\lambda = 4\pi$ and 8π respectively [Eq. (25)].

Now if we roughly connect $\hat{q} \propto s/\eta$ at $B = 0$ and $\hat{q}_{\parallel,\perp} \propto s/\eta_{\parallel,\perp}$ at $B \neq 0$, then we may write:

$$\begin{aligned} \frac{\hat{q}_{\parallel}(B)}{\hat{q}(B=0)} &= \frac{s/\eta_{\parallel}}{s/\eta} = \frac{47.5}{\left[16 + \frac{7}{8}12 \sum_{u,d,s} \frac{1}{1+(\tau_c/\tau_B)^2}\right]} \\ \frac{\hat{q}_{\perp}(B)}{\hat{q}(B=0)} &= \frac{s/\eta_{\perp}}{s/\eta} = \frac{47.5}{\left[16 + \frac{7}{8}12 \sum_{u,d,s} \frac{1}{1+4(\tau_c/\tau_B)^2}\right]}. \end{aligned} \quad (23)$$

Now realizing $\hat{q}(B=0)$ in terms of a simple quasi-particle form either $\hat{q}(B=0) = g(T) \times 5.87T^3$ from Eq. (11) or $\hat{q}(B=0) = g(T) \times \hat{q}_0$ from Eq. (13), we can express $\hat{q}_{\parallel,\perp}(T, B)$ as:

$$\begin{aligned} \hat{q}_{\parallel}(T, B) &= \frac{47.5}{\left[16 + \frac{7}{8}12 \sum_{u,d,s} \frac{1}{1+(\tau_c/\tau_B)^2}\right]} \times \left[g(T) \times 5.87T^3 \text{ or } g(T)\hat{q}_0\right] \\ \hat{q}_{\perp}(T, B) &= \frac{47.5}{\left[16 + \frac{7}{8}12 \sum_{u,d,s} \frac{1}{1+4(\tau_c/\tau_B)^2}\right]} \times \left[g(T) \times 5.87T^3 \text{ or } g(T)\hat{q}_0\right]. \end{aligned} \quad (24)$$

For more rich B -dependent structure, we can replace $g(T)$ by $g(T, B)$.

5 Results and discussions

In this section, we discuss the results for the estimation of \hat{q} numerically using quasi-particle model. Figure. (3) shows the temperature dependence of \hat{q}/T^3 in absence of magnetic field and the comparison with some of the earlier results [46, 64–71]. We notice that the result obtained using Eq. (11) (\hat{q}_N -based) is quite close with the calculation based on pQCD + HTL approximation [64]. So, we

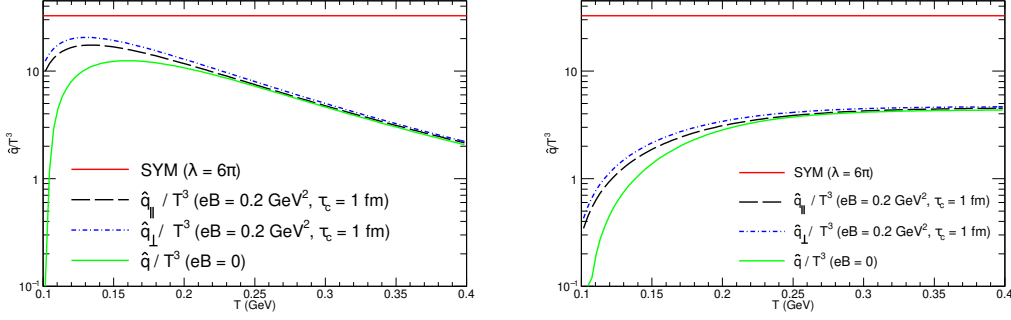


Figure 4: Dependence of \hat{q}/T^3 on temperature (T in GeV) — $\hat{q}_{\parallel,\perp}/T^3$ (black dash line and blue dash-dotted line) at $eB = 0.2 \text{ GeV}^2$, $\tau_c = 1 \text{ fm}$ and \hat{q}/T^3 at $eB = 0$ (green solid line) using Eq. (23) & (13) (Left panel) and using Eq. (23) & (11) (Right panel). Red solid line represents \hat{q} of an isotropic $\mathcal{N} = 4$ SYM plasma at zero magnetic field for $\lambda = 6\pi$ [Eq. (25)].

may relate our \hat{q}_N -based estimation with a weakly coupled QGP system as traditionally described by pQCD calculation, which works well only for weak coupling constant. On the other hand, to incorporate the non-pQCD outcome, semi-QGP + magnetic monopoles results [46] are also shown which are quite enhanced than HTL results. This non-pQCD estimation corresponds to strongly coupled system and our estimation from Eq. (13) (\hat{q}_0 -based) is found to follow similar trend. Both have a peak structure near transition temperatures of their respective models and also their peak strengths are close to the boundary, predicted for $\mathcal{N} = 4$ SYM plasma. In the absence of magnetic field, the jet quenching parameter for an isotropic $\mathcal{N} = 4$ SYM plasma has the form [72] : $\hat{q}_0 = \frac{\pi^{\frac{3}{2}} \Gamma(\frac{3}{4})}{\Gamma(\frac{5}{4})} \sqrt{\lambda} T^3$,

where $\sqrt{\lambda} = \sqrt{g_{YM}^2 N_c}$ with g_{YM} denoting the coupling strength of the strongly coupled plasma with color degeneracy factor N_c . The black dash-dotted line and solid line in Fig. (3) denote $\lambda = 4\pi$ and 8π respectively. Therefore, estimations of Eq. (11) and (13) may be considered as order of strength of \hat{q} for weakly and strongly coupled systems respectively. It is a quite interesting finding that by playing with existing experimental knowledge of jet quenching parameter for cold nuclear matter ($\hat{q}_N \approx 0.02 \text{ GeV}^2/\text{fm}$ [28, 29]) and hot QGP ($\hat{q}_0 \approx 0.9 \text{ GeV}^2/\text{fm}$ [27]), we are getting two directional aspects of QCD matter. When we are approaching from hadronic to QGP phase with \hat{q}_N , we are getting results close to weakly coupled QGP system. On the other hand, when we are approaching from QGP to hadronic phase with \hat{q}_0 , we are getting results close to strongly coupled QGP system. Interestingly, a cross-over type LQCD based temperature dependent gluon density is used for both cases.

Next, we have considered the effect of finite magnetic field on \hat{q}/T^3 . As mentioned in Refs. [44–48], there exists a correspondence between s/η and \hat{q}/T^3 . On this basis, we can have the equivalence of phase space in both quantities. In presence of magnetic field, η/s splits into parallel and perpendicular components which can be connected to the corresponding components of jet quenching parameter as shown in Eq. (23) and (24). Due to magnetic field a cyclotron motion of charged particles introduces a time scale τ_B (inverse of cyclotron frequency) along with the relaxation time τ_c which collectively constitute the phase space part in η/s as given in Eq. (18). The derived results from Eq. (24) are shown in Fig. 4 which invoke/incorporate the same phase space. The temperature dependence of \hat{q}/T^3 and its components at $eB = 0.2 \text{ GeV}^2$, $\tau_c = 1 \text{ fm}$ are shown. The red solid lines in both figures denote \hat{q} of an isotropic $\mathcal{N} = 4$ SYM plasma at zero magnetic field by putting $\lambda = 6\pi$ in Eq. (25). In presence of magnetic field, the components get enhanced and the difference between the two components decreases with increasing T due to the phase space part. If one analyzes details anatomy of \hat{q}/T^3 expression in Eq. (24), then we can identify two sources of B -dependence compo-

nents. One is B -dependent degeneracy factor, for which jet quenching parameter will be enhanced and another is phase-space part made of τ_B , for which jet quenching parameter will be enhanced further.

This impact of magnetic field on \hat{q} might be very challenging to observe experimentally however one can think of measuring nuclear suppression factor R_{AA} separately for quark and gluon initiated jets. The quark being charged will be affected by presence of magnetic field while gluon will not. Therefore, if one can design the experiment for these two separate measurements, then difference between two measurements can be linked with this B -dependent jet quenching parameter.

6 Aspects from ADS/CFT

The jet quenching parameter \hat{q} for the strongly coupled QCD plasma in the presence of a magnetic field has also been computed directly using the non-perturbative toolbox of AdS/CFT correspondence [73–78].

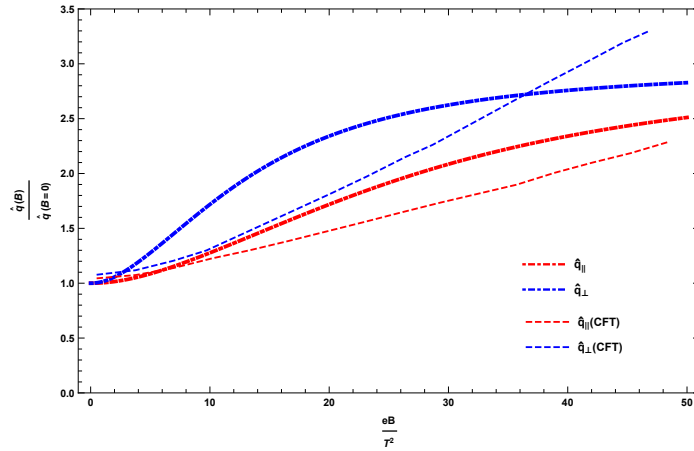


Figure 5: Comparison of the results for the ratio of $\hat{q}(B)$ to $\hat{q}(B = 0)$ obtained from the quasi-particle like approach against AdS/CFT techniques. The results for the quasi-particle approach are shown as thick dash-dotted lines and those from AdS/CFT are shown by the dashed lines. The above results are shown for $T = 0.3\text{GeV}$ and $\tau_c = 1\text{fm}$.

In fact, it has been shown that the magnitude of $\hat{q}(B = 0)$ calculated via AdS/CFT correspondence is closer to that extracted from RHIC data [79, 80] in comparison to the pQCD result. If we consider a magnetic field along the z -direction, the parton that forms the jet while traversing the medium can suffer a momentum broadening either along or transverse to the magnetic field direction, giving rise to three different components of jet quenching parameter: $\hat{q}_{||(\perp)}$, $\hat{q}_{\perp(||)}$ and $\hat{q}_{\perp(\perp)}$, where $\hat{q}_{||} \equiv \hat{q}_{||(\perp)}$ and $\hat{q}_{\perp} \equiv \hat{q}_{\perp(||)} + \hat{q}_{\perp(\perp)}$. In this notation, the first symbol denotes the direction of the magnetic field and the second denotes the direction in which the momentum broadening of the jet occurs. The result for these distinct \hat{q} values as obtained in Ref. [77] are

$$\hat{q}_{||(\perp)} = \frac{4\sqrt{\lambda}BT}{3\log(B/T^2)}, \quad (25)$$

$$\hat{q}_{\perp(||)} = \frac{2\pi}{3}\sqrt{\lambda}\sqrt{B}T^2, \quad (26)$$

and

$$\hat{q}_{\perp(\perp)} = \frac{\sqrt{\lambda}B^{3/2}}{3\pi\log(B/T^2)}. \quad (27)$$

From these results, one finds that in general the jet quenching parameter is enhanced in the presence of a magnetic field in comparison to the isotropic SYM case. Moreover, one gets $\hat{q}_{\perp(\perp)} > \hat{q}_{\parallel(\perp)} > \hat{q}_{\perp(\parallel)} > \hat{q}_0$ which shows that the values of the jet quenching parameter depends strongly on the direction of the moving quark as well as the direction in which the momentum broadening occurs.

We find an interesting comparison for the ratio $\frac{\hat{q}(B)}{\hat{q}(B=0)}$ obtained in Eq. (23) against the Ads/CFT results outlined above, for values of $\frac{eB}{T^2}$ upto 50, shown in Fig. (5). Both have found $\hat{q}_{\perp} > \hat{q}_{\parallel}$ and support enhance trend of quenching parameter in presence of magnetic field, although exact quantitative comparison might not be so good. A better upgradation of our present estimation can be possible by using the quantum aspect of magnetic field, where phase space will be proportional to eB due to Landau quantization. In that picture, we might get a proportional eB -dependence as we grossly notice for Ads/CFT results.

7 Summary

In summary, we have estimated the jet quenching parameter, \hat{q} in absence and presence of magnetic field using quasi-particle model where temperature and magnetic field dependent degeneracy factors of partons are considered for fitting the magneto-thermodynamical data of lattice quantum chromodynamics. Using the parametric degeneracy factor we have estimated the temperature (T) dependent gluon density to obtain $\hat{q}(T)$ from hadronic to QGP phase by restricting low and high temperature values of \hat{q} by their standard experimental values. During the restriction by low temperature cold nuclear matter data, temperature dependent $\hat{q}(T)$ from hadron to QGP phase become quite close to hard thermal loop or perturbative QCD results, which indicate transportation of jet in weakly interacting gas. While $\hat{q}(T)$ estimation from QGP to hadron phase is close to earlier estimations, which correspond to strongly interacting liquid picture.

Next, we go for the calculation of jet transport coefficient at finite magnetic field. Here, \hat{q} splits into parallel and perpendicular components, whose magnetic field dependent part has two sources. One is field dependent degeneracy factor and another is phase space part, guided from shear viscosity to entropy density ratio. The value of jet transport coefficients is found to be enhanced due to the collective role of these two sources. These results provide an additional information towards our current understanding and phenomenology of jet quenching in presence of magnetic field. Experimentally measurement and comparison of quark and gluon initiated jet suppression could possibly shed more light into it as the former being charged is expected to experience the effect of magnetic field while the latter does not.

Acknowledgment: The authors acknowledge to few members of TPRC-IITBH - Sarthak Satapathy, Jayanta Dey, Anki Anand, Ranjesh Kumar, Ankita Mishra, Prasant Murmu, who worked on quasi-particle picture [35, 58], which is used in present work. D. Banerjee acknowledges Inspire Fellowship research grant [DST/INSPIRE Fellowship/2018/IF180285]. A. Modak and P. Das acknowledge Institutional Fellowship research grant of Bose Institute. A. Budh Raja thanks to Dr. Rishi Sharma for useful discussion.

References

- [1] Megan Connors et al. “Jet measurements in heavy ion physics”. In: *Rev. Mod. Phys.* 90 (2018), p. 025005. DOI: 10.1103/RevModPhys.90.025005. arXiv: 1705.01974 [nucl-ex].
- [2] Abelev et al. “Charged jet cross sections and properties in proton-proton collisions at $\sqrt{s} = 7$ TeV”. In: *Phys. Rev. D* 91 (11 June 2015), p. 112012. DOI: 10.1103/PhysRevD.91.112012. URL: <https://link.aps.org/doi/10.1103/PhysRevD.91.112012>.

- [3] Chatrchyan et al. “Measurement of the Inclusive Jet Cross Section in pp Collisions at $\sqrt{s} = 7$ TeV”. In: *Phys. Rev. Lett.* 107 (13 Sept. 2011), p. 132001. DOI: 10.1103/PhysRevLett.107.132001. URL: <https://link.aps.org/doi/10.1103/PhysRevLett.107.132001>.
- [4] B. Abelev et al. “Measurement of the inclusive differential jet cross section in pp collisions at $\sqrt{s} = 2.76$ TeV”. In: *Physics Letters B* 722.4 (2013), pp. 262–272. ISSN: 0370-2693. DOI: <https://doi.org/10.1016/j.physletb.2013.04.026>. URL: <https://www.sciencedirect.com/science/article/pii/S0370269313003055>.
- [5] F. Abe et al. “A Measurement of jet shapes in $p\bar{p}$ collisions at $\sqrt{s} = 1.8$ TeV”. In: *Phys. Rev. Lett.* 70 (1993), pp. 713–717. DOI: 10.1103/PhysRevLett.70.713.
- [6] Georges Aad et al. “Measurement of the jet fragmentation function and transverse profile in proton-proton collisions at a center-of-mass energy of 7 TeV with the ATLAS detector”. In: *Eur. Phys. J. C* 71 (2011), p. 1795. DOI: 10.1140/epjc/s10052-011-1795-y. arXiv: 1109.5816 [hep-ex].
- [7] Jaroslav Adam et al. “Centrality dependence of charged jet production in p-Pb collisions at $\sqrt{s_{NN}} = 5.02$ TeV”. In: *Eur. Phys. J. C* 76.5 (2016), p. 271. DOI: 10.1140/epjc/s10052-016-4107-8. arXiv: 1603.03402 [nucl-ex].
- [8] I. Ya. Aref’eva. “Formation time of quark–gluon plasma in heavy-ion collisions in the holographic shock wave model”. In: *Teor. Mat. Fiz.* 184.3 (2015), pp. 398–417. DOI: 10.1007/s11232-015-0331-x. arXiv: 1503.02185 [hep-th].
- [9] Rupa Chatterjee et al. “Formation Time of QGP from Thermal Photon Elliptic Flow”. In: *Nucl. Phys. A* 830 (2009). Ed. by Paul Stankus et al., pp. 503C–506C. DOI: 10.1016/j.nuclphysa.2009.10.043. arXiv: 0907.3548 [nucl-th].
- [10] Miklos Gyulassy et al. “Jet Quenching in Dense Matter”. In: *Phys. Lett. B* 243 (1990), pp. 432–438. DOI: 10.1016/0370-2693(90)91409-5.
- [11] Xin-Nian Wang et al. “Gluon shadowing and jet quenching in A + A collisions at $\sqrt{s_{NN}} = 200$ GeV”. In: *Phys. Rev. Lett.* 68 (1992), pp. 1480–1483. DOI: 10.1103/PhysRevLett.68.1480.
- [12] A. Majumder et al. “The Theory and Phenomenology of Perturbative QCD Based Jet Quenching”. In: *Prog. Part. Nucl. Phys.* 66 (2011), pp. 41–92. DOI: 10.1016/j.ppnp.2010.09.001. arXiv: 1002.2206 [hep-ph].
- [13] Karen M. Burke et al. “Extracting the jet transport coefficient from jet quenching in high-energy heavy-ion collisions”. In: *Phys. Rev. C* 90.1 (2014), p. 014909. DOI: 10.1103/PhysRevC.90.014909. arXiv: 1312.5003 [nucl-th].
- [14] Andras Laszlo. “Nuclear modification at $\sqrt{s_{NN}} = 17.3$ GeV, measured at NA49”. In: *Indian J. Phys.* 85 (2011). Ed. by Jan-e Alam et al., pp. 787–791. DOI: 10.1007/s12648-011-0077-8. arXiv: 0805.4771 [nucl-ex].
- [15] Adare et al. “Transverse momentum dependence of η meson suppression in Au+Au collisions at $\sqrt{s_{NN}} = 200$ GeV”. In: *Phys. Rev. C* 82 (1 July 2010), p. 011902. DOI: 10.1103/PhysRevC.82.011902. URL: <https://link.aps.org/doi/10.1103/PhysRevC.82.011902>.
- [16] Serguei Chatrchyan et al. “Study of high-pT charged particle suppression in PbPb compared to pp collisions at $\sqrt{s_{NN}} = 2.76$ TeV”. In: *Eur. Phys. J. C* 72 (2012), p. 1945. DOI: 10.1140/epjc/s10052-012-1945-x. arXiv: 1202.2554 [nucl-ex].
- [17] Vardan Khachatryan et al. “Measurement of inclusive jet production and nuclear modifications in pPb collisions at $\sqrt{s_{NN}} = 5.02$ TeV”. In: *Eur. Phys. J. C* 76.7 (2016), p. 372. DOI: 10.1140/epjc/s10052-016-4205-7. arXiv: 1601.02001 [nucl-ex].
- [18] B. Abelev et al. “Measurement of charged jet suppression in Pb-Pb collisions at $\sqrt{s_{NN}} = 2.76$ TeV”. In: *JHEP* 03 (2014), p. 013. DOI: 10.1007/JHEP03(2014)013. arXiv: 1311.0633 [nucl-ex].

- [19] M. Gyulassy et al. “Reaction operator approach to nonAbelian energy loss”. In: *Nucl. Phys. B* 594 (2001), pp. 371–419. DOI: 10.1016/S0550-3213(00)00652-0. arXiv: nucl-th/0006010.
- [20] Ivan Vitev et al. “High- p_T Tomography of $d + \text{Au}$ and $\text{Au} + \text{Au}$ at SPS, RHIC, and LHC”. In: *Phys. Rev. Lett.* 89 (25 Dec. 2002), p. 252301. DOI: 10.1103/PhysRevLett.89.252301. URL: <https://link.aps.org/doi/10.1103/PhysRevLett.89.252301>.
- [21] Alessandro Buzzatti et al. “Jet Flavor Tomography of Quark Gluon Plasmas at RHIC and LHC”. In: *Phys. Rev. Lett.* 108 (2 Jan. 2012), p. 022301. DOI: 10.1103/PhysRevLett.108.022301. URL: <https://link.aps.org/doi/10.1103/PhysRevLett.108.022301>.
- [22] Björn Schenke et al. “MARTINI: An event generator for relativistic heavy-ion collisions”. In: *Phys. Rev. C* 80 (5 Nov. 2009), p. 054913. DOI: 10.1103/PhysRevC.80.054913. URL: <https://link.aps.org/doi/10.1103/PhysRevC.80.054913>.
- [23] Guang-You Qin et al. “Radiative and Collisional Jet Energy Loss in the Quark-Gluon Plasma at the BNL Relativistic Heavy Ion Collider”. In: *Phys. Rev. Lett.* 100 (7 Feb. 2008), p. 072301. DOI: 10.1103/PhysRevLett.100.072301. URL: <https://link.aps.org/doi/10.1103/PhysRevLett.100.072301>.
- [24] Abhijit Majumder. “Hard collinear gluon radiation and multiple scattering in a medium”. In: *Phys. Rev. D* 85 (1 Jan. 2012), p. 014023. DOI: 10.1103/PhysRevD.85.014023. URL: <https://link.aps.org/doi/10.1103/PhysRevD.85.014023>.
- [25] Xiaofeng Guo et al. “Multiple Scattering, Parton Energy Loss, and Modified Fragmentation Functions in Deeply Inelastic eA Scattering”. In: *Phys. Rev. Lett.* 85 (17 Oct. 2000), pp. 3591–3594. DOI: 10.1103/PhysRevLett.85.3591. URL: <https://link.aps.org/doi/10.1103/PhysRevLett.85.3591>.
- [26] Xin-Nian Wang et al. “Multiple parton scattering in nuclei: parton energy loss”. In: *Nuclear Physics A* 696.3 (2001), pp. 788–832. ISSN: 0375-9474. DOI: [https://doi.org/10.1016/S0375-9474\(01\)01130-7](https://doi.org/10.1016/S0375-9474(01)01130-7). URL: <https://www.sciencedirect.com/science/article/pii/S0375947401011307>.
- [27] Xiao-Fang Chen et al. “Bulk matter evolution and extraction of jet transport parameters in heavy-ion collisions at energies available at the BNL Relativistic Heavy Ion Collider (RHIC)”. In: *Phys. Rev. C* 81 (6 June 2010), p. 064908. DOI: 10.1103/PhysRevC.81.064908. URL: <https://link.aps.org/doi/10.1103/PhysRevC.81.064908>.
- [28] A. Airapetian et al. “Hadronization in semi-inclusive deep-inelastic scattering on nuclei”. In: *Nucl. Phys. B* 780 (2007), pp. 1–27. DOI: 10.1016/j.nuclphysb.2007.06.004. arXiv: 0704.3270 [hep-ex].
- [29] Wei-Tian Deng et al. “Multiple parton scattering in nuclei: Modified Dokshitzer-Gribov-Lipatov-Altarelli-Parisi (DGLAP) evolution for fragmentation functions”. In: *Phys. Rev. C* 81 (2 Feb. 2010), p. 024902. DOI: 10.1103/PhysRevC.81.024902. URL: <https://link.aps.org/doi/10.1103/PhysRevC.81.024902>.
- [30] A. Adare et al. “Suppression Pattern of Neutral Pions at High Transverse Momentum in $\text{Au} + \text{Au}$ Collisions at $\sqrt{s_{NN}} = 200$ GeV and Constraints on Medium Transport Coefficients”. In: *Phys. Rev. Lett.* 101 (23 Dec. 2008), p. 232301. DOI: 10.1103/PhysRevLett.101.232301. URL: <https://link.aps.org/doi/10.1103/PhysRevLett.101.232301>.
- [31] A. Adare et al. “Neutral pion production with respect to centrality and reaction plane in $\text{Au} + \text{Au}$ collisions at $\sqrt{s_{NN}} = 200$ GeV”. In: *Phys. Rev. C* 87 (3 Mar. 2013), p. 034911. DOI: 10.1103/PhysRevC.87.034911. URL: <https://link.aps.org/doi/10.1103/PhysRevC.87.034911>.
- [32] Betty Abelev et al. “Centrality Dependence of Charged Particle Production at Large Transverse Momentum in Pb–Pb Collisions at $\sqrt{s_{NN}} = 2.76$ TeV”. In: *Phys. Lett. B* 720 (2013), pp. 52–62. DOI: 10.1016/j.physletb.2013.01.051. arXiv: 1208.2711 [hep-ex].

- [33] Serguei Chatrchyan et al. “Study of high-pT charged particle suppression in PbPb compared to pp collisions at $\sqrt{s_{NN}} = 2.76$ TeV”. In: *Eur. Phys. J. C* 72 (2012), p. 1945. DOI: 10.1140/epjc/s10052-012-1945-x. arXiv: 1202.2554 [nucl-ex].
- [34] Kirill Tuchin. “Particle production in strong electromagnetic fields in relativistic heavy-ion collisions”. In: *Adv. High Energy Phys.* 2013 (2013), p. 490495. DOI: 10.1155/2013/490495. arXiv: 1301.0099 [hep-ph].
- [35] Sarthak Satapathy et al. “From Non-interacting to Interacting Picture of Thermodynamics and Transport Coefficients for Quark Gluon Plasma”. In: *J. Phys. G* 47.4 (2020), p. 045201. DOI: 10.1088/1361-6471/ab614d. arXiv: 1908.04330 [hep-ph].
- [36] Szabolcs Borsányi et al. “Full result for the QCD equation of state with 2+1 flavors”. In: *Physics Letters B* 730 (2014), pp. 99–104. ISSN: 0370-2693. DOI: <https://doi.org/10.1016/j.physletb.2014.01.007>. URL: <https://www.sciencedirect.com/science/article/pii/S0370269314000197>.
- [37] A. Bazavov et al. “Equation of state in $(2 + 1)$ -flavor QCD”. In: *Phys. Rev. D* 90 (9 Nov. 2014), p. 094503. DOI: 10.1103/PhysRevD.90.094503. URL: <https://link.aps.org/doi/10.1103/PhysRevD.90.094503>.
- [38] G. S. Bali et al. “QCD quark condensate in external magnetic fields”. In: *Phys. Rev. D* 86 (7 Oct. 2012), p. 071502. DOI: 10.1103/PhysRevD.86.071502. URL: <https://link.aps.org/doi/10.1103/PhysRevD.86.071502>.
- [39] G. S. Bali et al. “The QCD equation of state in background magnetic fields”. In: *JHEP* 08 (2014), p. 177. DOI: 10.1007/JHEP08(2014)177. arXiv: 1406.0269 [hep-lat].
- [40] Xiang Li et al. “Thermodynamics of $2 + 1$ flavor Polyakov-loop quark-meson model under external magnetic field”. In: *Phys. Rev. D* 99 (7 Apr. 2019), p. 074029. DOI: 10.1103/PhysRevD.99.074029. URL: <https://link.aps.org/doi/10.1103/PhysRevD.99.074029>.
- [41] Abdel Nasser Tawfik et al. “Quark–hadron phase structure, thermodynamics, and magnetization of QCD matter”. In: *J. Phys. G* 45.5 (2018), p. 055008. DOI: 10.1088/1361-6471/aaba9e. arXiv: 1604.08174 [hep-lat].
- [42] Abdel Nasser Tawfik et al. “QCD thermodynamics and magnetization in nonzero magnetic field”. In: *Adv. High Energy Phys.* 2016 (2016), p. 1381479. DOI: 10.1155/2016/1381479. arXiv: 1604.00043 [hep-ph].
- [43] R. L. S. Farias et al. “Thermo-magnetic effects in quark matter: Nambu–Jona-Lasinio model constrained by lattice QCD”. In: *Eur. Phys. J. A* 53.5 (2017), p. 101. DOI: 10.1140/epja/i2017-12320-8. arXiv: 1603.03847 [hep-ph].
- [44] Abhijit Majumder et al. “Small Shear Viscosity of a Quark-Gluon Plasma Implies Strong Jet Quenching”. In: *Phys. Rev. Lett.* 99 (19 Nov. 2007), p. 192301. DOI: 10.1103/PhysRevLett.99.192301. URL: <https://link.aps.org/doi/10.1103/PhysRevLett.99.192301>.
- [45] Jorge Casalderrey-Solana et al. “Energy dependence of jet transport parameter and parton saturation in quark-gluon plasma”. In: *Phys. Rev. C* 77 (2 Feb. 2008), p. 024902. DOI: 10.1103/PhysRevC.77.024902. URL: <https://link.aps.org/doi/10.1103/PhysRevC.77.024902>.
- [46] Jiechen Xu et al. “Consistency of Perfect Fluidity and Jet Quenching in Semi-Quark-Gluon Monopole Plasmas”. In: *Chinese Physics Letters* 32.9 (Aug. 2015), p. 092501. DOI: 10.1088/0256-307x/32/9/092501. URL: <https://doi.org/10.1088/0256-307x/32/9/092501>.
- [47] Jiechen Xu et al. “Bridging Soft-Hard Transport Properties of Quark-Gluon Plasmas with CUJET3.0”. In: *JHEP* 02 (2016), p. 169. DOI: 10.1007/JHEP02(2016)169. arXiv: 1508.00552 [hep-ph].

- [48] Edward Shuryak. “Strongly coupled quark-gluon plasma in heavy ion collisions”. In: *Rev. Mod. Phys.* 89 (3 July 2017), p. 035001. DOI: 10.1103/RevModPhys.89.035001. URL: <https://link.aps.org/doi/10.1103/RevModPhys.89.035001>.
- [49] Alejandro Ayala et al. “Relating \hat{q} , η/s , and ΔE in an expanding quark-gluon plasma”. In: *Phys. Rev. C* 94 (2 Aug. 2016), p. 024913. DOI: 10.1103/PhysRevC.94.024913. URL: <https://link.aps.org/doi/10.1103/PhysRevC.94.024913>.
- [50] E.M. Lifshitz et al. *Physical Kinetics*. Elsevier India, 1981. ISBN: 978-0-08-057049-5. DOI: 10.1016/C2009-0-25523-1.
- [51] Xu-Guang Huang et al. “Anisotropic hydrodynamics, bulk viscosities, and r -modes of strange quark stars with strong magnetic fields”. In: *Phys. Rev. D* 81 (4 Feb. 2010), p. 045015. DOI: 10.1103/PhysRevD.81.045015. URL: <https://link.aps.org/doi/10.1103/PhysRevD.81.045015>.
- [52] Xu-Guang Huang et al. “Kubo formulae for relativistic fluids in strong magnetic fields”. In: *Annals Phys.* 326 (2011), pp. 3075–3094. DOI: 10.1016/j.aop.2011.08.001. arXiv: 1108.0602 [astro-ph.HE].
- [53] Kirill Tuchin. “On viscous flow and azimuthal anisotropy of quark-gluon plasma in strong magnetic field”. In: *J. Phys. G* 39 (2012), p. 025010. DOI: 10.1088/0954-3899/39/2/025010. arXiv: 1108.4394 [nucl-th].
- [54] Shiyong Li et al. “Shear viscosity of the quark-gluon plasma in a weak magnetic field in perturbative QCD: Leading log”. In: *Phys. Rev. D* 97.5 (2018), p. 056024. DOI: 10.1103/PhysRevD.97.056024. arXiv: 1707.00795 [hep-ph].
- [55] Payal Mohanty et al. “One particle distribution function and shear viscosity in magnetic field: a relaxation time approach”. In: *Eur. Phys. J. A* 55 (2019), p. 35. DOI: 10.1140/epja/i2019-12705-7. arXiv: 1804.01788 [nucl-th].
- [56] Sabyasachi Ghosh et al. “Impact of magnetic field on shear viscosity of quark matter in Nambu–Jona-Lasinio model”. In: *Phys. Rev. D* 100.3 (2019), p. 034024. DOI: 10.1103/PhysRevD.100.034024. arXiv: 1804.00812 [hep-ph].
- [57] Seung-il Nam et al. “Shear viscosity of quark matter at finite temperature under an external magnetic field”. In: *Phys. Rev. D* 87 (11 June 2013), p. 114003. DOI: 10.1103/PhysRevD.87.114003. URL: <https://link.aps.org/doi/10.1103/PhysRevD.87.114003>.
- [58] Jayanta Dey et al. “From Non-interacting to Interacting Picture of Quark Gluon Plasma in presence of magnetic field and its fluid property”. In: (Aug. 2019). arXiv: 1908.04335 [hep-ph].
- [59] Ashutosh Dash et al. “Anisotropic transport properties of a hadron resonance gas in a magnetic field”. In: *Phys. Rev. D* 102.1 (2020), p. 016016. DOI: 10.1103/PhysRevD.102.016016. arXiv: 2002.08781 [nucl-th].
- [60] Arpan Das et al. “Transport coefficients of hot and dense hadron gas in a magnetic field: A relaxation time approach”. In: *Phys. Rev. D* 100 (11 Dec. 2019), p. 114004. DOI: 10.1103/PhysRevD.100.114004. URL: <https://link.aps.org/doi/10.1103/PhysRevD.100.114004>.
- [61] Gabriel S. Denicol et al. “Nonresistive dissipative magnetohydrodynamics from the Boltzmann equation in the 14-moment approximation”. In: *Phys. Rev. D* 98 (7 Oct. 2018), p. 076009. DOI: 10.1103/PhysRevD.98.076009. URL: <https://link.aps.org/doi/10.1103/PhysRevD.98.076009>.
- [62] Zhengyu Chen et al. “Calculation of anisotropic transport coefficients for an ultrarelativistic Boltzmann gas in a magnetic field within a kinetic approach”. In: *Phys. Rev. D* 101 (5 Mar. 2020), p. 056020. DOI: 10.1103/PhysRevD.101.056020. URL: <https://link.aps.org/doi/10.1103/PhysRevD.101.056020>.

- [63] Jayanta Dey et al. “Shear viscosity and electrical conductivity of relativistic fluid in presence of magnetic field: a massless case”. In: (July 2019). arXiv: 1907.11164 [hep-ph].
- [64] Jiechen Xu et al. “Azimuthal jet flavor tomography with CUJET2.0 of nuclear collisions at RHIC and LHC”. In: *JHEP* 08 (2014), p. 063. DOI: 10.1007/JHEP08(2014)063. arXiv: 1402.2956 [hep-ph].
- [65] Yoshimasa Hidaka et al. “Suppression of the shear viscosity in a “semi”-quark-gluon plasma”. In: *Phys. Rev. D* 78 (7 Oct. 2008), p. 071501. DOI: 10.1103/PhysRevD.78.071501. URL: <https://link.aps.org/doi/10.1103/PhysRevD.78.071501>.
- [66] Yoshimasa Hidaka et al. “Small shear viscosity in the semiquark gluon plasma”. In: *Phys. Rev. D* 81 (7 Apr. 2010), p. 076002. DOI: 10.1103/PhysRevD.81.076002. URL: <https://link.aps.org/doi/10.1103/PhysRevD.81.076002>.
- [67] Adrian Dumitru et al. “How wide is the transition to deconfinement?” In: *Phys. Rev. D* 83 (3 Feb. 2011), p. 034022. DOI: 10.1103/PhysRevD.83.034022. URL: <https://link.aps.org/doi/10.1103/PhysRevD.83.034022>.
- [68] Shu Lin et al. “Collisional energy loss above the critical temperature in QCD”. In: *Physics Letters B* 730 (2014), pp. 236–242. ISSN: 0370-2693. DOI: <https://doi.org/10.1016/j.physletb.2014.01.043>. URL: <https://www.sciencedirect.com/science/article/pii/S0370269314000653>.
- [69] Jinfeng Liao et al. “Strongly coupled plasma with electric and magnetic charges”. In: *Phys. Rev. C* 75 (5 May 2007), p. 054907. DOI: 10.1103/PhysRevC.75.054907. URL: <https://link.aps.org/doi/10.1103/PhysRevC.75.054907>.
- [70] Jinfeng Liao et al. “The Magnetic Component of Quark-Gluon Plasma is also a Liquid”. In: *Phys. Rev. Lett.* 101 (16 Oct. 2008), p. 162302. DOI: 10.1103/PhysRevLett.101.162302. URL: <https://link.aps.org/doi/10.1103/PhysRevLett.101.162302>.
- [71] Jinfeng Liao et al. “Effect of Light Fermions on the Confinement Transition in QCD-Like Theories”. In: *Phys. Rev. Lett.* 109 (15 Oct. 2012), p. 152001. DOI: 10.1103/PhysRevLett.109.152001. URL: <https://link.aps.org/doi/10.1103/PhysRevLett.109.152001>.
- [72] Hong Liu et al. “Calculating the Jet Quenching Parameter”. In: *Phys. Rev. Lett.* 97 (18 Nov. 2006), p. 182301. DOI: 10.1103/PhysRevLett.97.182301. URL: <https://link.aps.org/doi/10.1103/PhysRevLett.97.182301>.
- [73] Juan Martin Maldacena. “The Large N limit of superconformal field theories and supergravity”. In: *Adv. Theor. Math. Phys.* 2 (1998), pp. 231–252. DOI: 10.1023/A:1026654312961. arXiv: hep-th/9711200.
- [74] S. S. Gubser et al. “Gauge theory correlators from noncritical string theory”. In: *Phys. Lett. B* 428 (1998), pp. 105–114. DOI: 10.1016/S0370-2693(98)00377-3. arXiv: hep-th/9802109.
- [75] Ofer Aharony et al. “Large N field theories, string theory and gravity”. In: *Phys. Rept.* 323 (2000), pp. 183–386. DOI: 10.1016/S0370-1573(99)00083-6. arXiv: hep-th/9905111.
- [76] Shiyong Li et al. “Jet quenching parameter of the quark-gluon plasma in a strong magnetic field: Perturbative QCD and AdS/CFT correspondence”. In: *Phys. Rev. D* 94 (8 Oct. 2016), p. 085016. DOI: 10.1103/PhysRevD.94.085016. URL: <https://link.aps.org/doi/10.1103/PhysRevD.94.085016>.
- [77] Zi-qiang Zhang et al. “The effect of magnetic field on jet quenching parameter”. In: *Eur. Phys. J. C* 78.7 (2018), p. 532. DOI: 10.1140/epjc/s10052-018-6019-2.
- [78] Kiminad A. Mamo. “Inverse magnetic catalysis in holographic models of QCD”. In: *JHEP* 05 (2015), p. 121. DOI: 10.1007/JHEP05(2015)121. arXiv: 1501.03262 [hep-th].

- [79] K. J. Eskola et al. “The Fragility of high-p(T) hadron spectra as a hard probe”. In: *Nucl. Phys. A* 747 (2005), pp. 511–529. DOI: 10.1016/j.nuclphysa.2004.09.070. arXiv: hep-ph/0406319.
- [80] A. Dainese et al. “Leading-particle suppression in high energy nucleus-nucleus collisions”. In: *Eur. Phys. J. C* 38 (2005), pp. 461–474. DOI: 10.1140/epjc/s2004-02077-x. arXiv: hep-ph/0406201.